



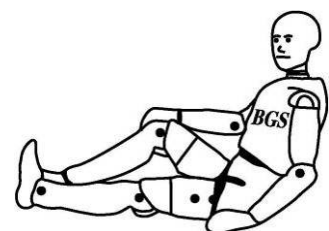
**Report**

**Flexible Pedestrian Legform Impactor**

**Influence Of Test Parameter Variations  
On The Flex-PLI**

**A Joint Project of  
ACEA - The European Automobile Manufacturer's Association  
and  
BAST - The German Federal Highway Research Institute**

Version: Draft 1  
Date: 09.03.2010  
Author: Dipl.-Ing. Dirk-Uwe Gehring  
BGS Böhme & Gehring GmbH



# Content

<b>1 Introduction</b> .....	<b>3</b>
<b>2 Test configuration</b> .....	<b>4</b>
2.1 Test Subject .....	4
2.2 Test Facility .....	5
2.3 Inverse Test Setup .....	6
2.4 Measurement System .....	7
2.5 Film and photo documentation .....	8
<b>3 Test Execution</b> .....	<b>8</b>
3.1 Inverse Tests.....	8
3.2 Parameter Variation .....	9
<b>4 Test Results</b> .....	<b>11</b>
<b>5 Evaluation of the Test Results</b> .....	<b>12</b>
5.1 Rotation around the Z-Axis.....	13
5.2 Impact Height Variation .....	14
5.3 Impact Velocity Variation.....	16
5.4 General Observations and Findings.....	17
<b>6 Conclusions</b> .....	<b>17</b>
<b>7 Annexes (DVD)</b> .....	<b>18</b>

# 1 Introduction

The Flexible Pedestrian Legform Impactor (Flex-PLI) is going to become the successor of the current legform impactor for worldwide use in tests to assess the pedestrian protection capabilities of vehicles. A corresponding amendment to the global technical regulation (gtr) no. 9 “Pedestrian Safety” has already been proposed. This proposal is expected to be accepted in one of the upcoming meetings of the UNECE WP29/GRSP<sup>1</sup>.

Several test programmes with the various development versions of the Flex-PLI have already been performed in order to evaluate the new impactor and to achieve some knowledge about its performance. Since the latest development version, the Flex GTR, is supposed to be the final version, it is essential to gain as many experience as possible with this impactor. Thus, in 2009, many tests have been performed in test labs in Japan, Europe and USA with the first prototypes of the Flex GTR. During one extensive evaluation test series as a joint project between ACEA and BAST it was even possible to use all three first prototypes to investigate especially repeatability and reproducibility in vehicle tests and in tests under idealized test conditions (“inverse tests”).

In order to further evaluate the impactor in detail and to be able to use it as a homologation test tool it is necessary to investigate the sensitivity of the impactor to test parameter variations.

As the legform impacts the vehicle in free flight, several test parameters need to be controlled. An impactor rotation may occur during the flight. The height of the impactor at first contact depends on the test speed and on the precise positioning of the vehicle in front of the test stand since the flight curve is a parabolic trajectory. Of course, the impact velocity could also vary from test to test, influencing the test results. At least, environment factors may affect the performance, too.

It is rather obvious that each of these parameters could have an influence on the test results but to be able to quantify the influences, a series of tests was conducted, investigating the effect of variation of the most significant test parameters: the yaw angle (rotation around z-axis), the impact height and the impact velocity.

The parameter variations were tested in an inverse test setup in which the impactor is hung from a releasable fixture and impacted by an aluminium honeycomb cuboid as this specific test setup offers the possibilities to realize the parameter variations under exactly controlled conditions.

---

<sup>1</sup> UNECE: United Nations Economic Commission for Europe  
WP29: World Forum for Harmonisation of Vehicle Regulations  
GRSP: Groupe de Rapporteurs sur la Sécurité Passive (Working Party on Passive Safety)

## 2 Test configuration

### 2.1 Test Subject

The GTR version of the Flex-PLI is the last version of the prototype legform and expected to be at least almost ready for use for regulatory purposes.

The Flex-GTR consists of flexible femur and tibia sections and a central knee joint. The inner structure is covered by a multilayer skin and flesh simulation, made of neoprene and rubber, whose outermost layer is a one-piece neoprene skin, which covers the whole length of the legform (see fig. 1).

The impactor measures 926 mm in length, weighs 12.4 kg and has a cross-section-dimension of 140 mm for the femur and 132 mm for the tibia section.

The femur is made of eight individual segments aligned on a central bone core, made of glass fibre reinforced plastic (GRP) simulating the human femur bone. The individual segments are held in place by metal brackets attached to their sides, keeping them flexibly aligned. The tibia is built similar to the femur but consists of ten segments. All segments are made of plastic, except for the ones at the upper and lower ends of femur and tibia, which are made of aluminium. Both femur and tibia are equipped with four steel cables with ball ends, guided through the edges of the segments, to limit the bending of the legform. At either end of the legform, plastic covers provide some protection to the end segments. The impact side of the legform is covered with rounded plastic mouldings. Figure 2 shows the whole impactor without flesh and skin simulation.



Fig. 1: Flex GTR

The knee assembly, manufactured from aluminium, consists of upper and lower halves, which are held together by twelve steel cables bedded in compound springs to limit bending and shearing of the knee. In the knee assembly, space is provided for the displacement sensors and an on-board data acquisition system. Figure 3 shows the disassembled knee joint of the impactor.

Figure 4 shows the three separated sections of the impactor: Femur, knee, tibia.

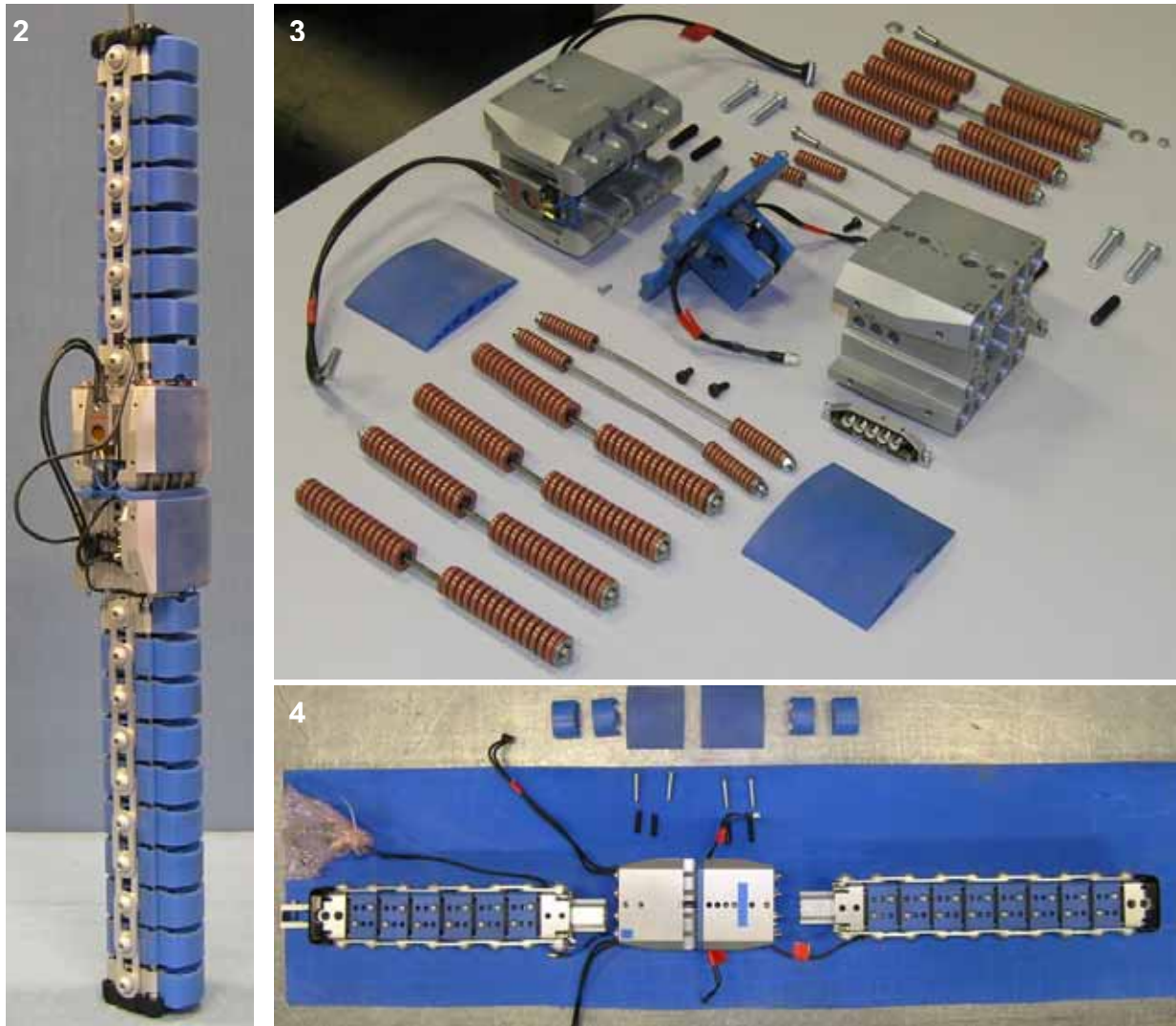


Fig. 2-4: Assembly pictures of the Flex GTR

The standard measurement equipment of the impactor consists of strain gauges in the femur and tibia and displacement sensors in the knee.

The knee displacements are measured by an arrangement of four position transducers: two string potentiometers for the cruciate ligaments (anterior and posterior) and another two for the collateral ligaments (medial and lateral).

The bending moments in the femur as well as in the tibia are measured by strain gauges mounted to the bone cores. There are three pairs of strain gauges located in the femur and four in the tibia of the impactor. Each pair consists of one strain gauge at the impact side and one at the non-impact side of the long bone.

## 2.2 Test Facility

The tests were conducted at the vehicle component test facility (FKTA) of the German Federal Highway Research Institute (BAST). BAST runs an accelerator of the type “Hydropropulsator”

built by IST GmbH, Germany (fig. 5). All of BAST's pedestrian protection tests as well as impactor certifications and other impact tests are conducted with this facility.



Fig. 5: Vehicle Component Test Facility of BAST

### 2.3 Inverse Test Setup



Fig. 6: Legform support rig for inverse tests

For the inverse test the catapult module with the piston rod of the test stand was adjusted horizontally and a linear guiding rig with flat impactor module was mounted to the catapult module.

An aluminium honeycomb was attached to the module face as an exchangeable, deformable impactor. To protect the legform skin, the honeycomb was wrapped tightly with paper.

To support the legform, a special test rig with quick release was placed in front of the test stand and fixed to the ground (fig. 6). The legform was attached to the rig using its guide-roller. The guide roller was positioned on a pin-jointed hook, which was pre-tensioned by a spring to enable a sudden release and to minimize the influence of the support on the test results.

Figure 7 shows the setup of the inverse tests.



Fig. 7: Inverse Test Setup

## 2.4 Measurement System

To record data of the tests the internal sensors of the impactor were used. The measurement system of the Flex-PLI consists of four string potentiometers to record knee displacements, seven strain gauges which record the bending moments on the longbones and an accelerometer mounted to the knee, which is only used for pendulum tests.

The position transducers of the type Space Age 170-0161 (datasheet see annex 5) are geometrically arranged to measure elongations in the positions of the Anterior Crucial Ligament (ACL), the Posterior Cruciate Ligament (PCL) as well as the Medial Collateral Ligament (MCL) and the Lateral Collateral Ligament (LCL).

The type of strain gauges on the longbones is Kyowa KFEL-5-350 (datasheet see annex 5). They are serially numbered from the knee to the ends: Tibia A1 to Tibia A4 and Femur: Femur A1 to Femur A3.

The measurement of the impact velocity was achieved using a calibrated light-barrier system by Hentschel GmbH, Germany, which consists of an infrared pulser with receiver and a counter.

The impact accuracy was documented by a paint spot.

## 2.5 Film and photo documentation

For every test a comprehensive photo documentation was made prior to and after the test. All of these photographs are included in annex 1 of this report.

In addition, a highspeed video camera was used to record an overview of the impact and to capture the whole trajectory of the legform in every test. For a better evaluation of the kinematics of some of the tests, a second camera was used in these cases. The recording frequency of the cameras was 1000 frames per second.

A complete file listing and all the high speed films are included in annex 2 of this report.

## 3 Test Execution

### 3.1 Inverse Tests

The general inverse test configuration is to vertically align the upper surface of the honeycomb with the middle of the knee joint. Horizontally the centreline of the honeycomb is aligned with the vertical axis of the legform impactor. This alignment was checked and adjusted if necessary before every test (fig. 8).

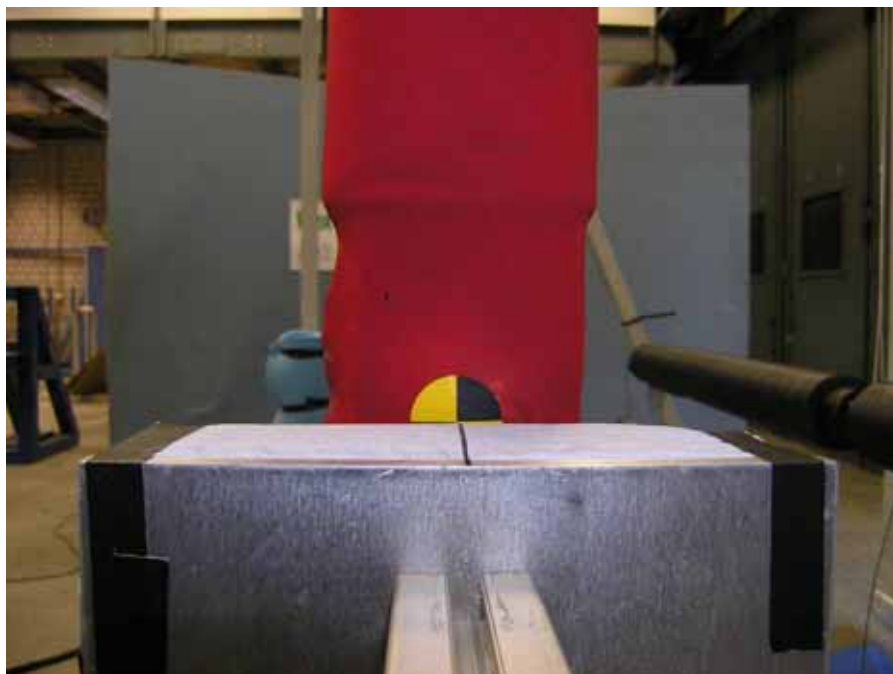


Fig. 8: General alignment of the honeycomb with the legform

For the variation of the impact height, the accelerator module with the honeycomb impactor was positioned further upwards or further downwards, respectively. The variation of the impact angle



was achieved by using modified brackets for the guide roller of the legform. These brackets were bent so that the legform was rotated either by  $-10^\circ$  or by  $+10^\circ$  around the z-axis (fig. 9).



Fig. 9: Modified support bracket for impact angle variation of  $+10^\circ$   
(view in impact direction)

The honeycombs were 250 mm wide, 160 mm high and 60 mm thick “Aluminium Honeycomb 3.1 3/16 5052” cuboids with a crush strength of 75 PSI according to the certificate of the manufacturer, Cellbond Composites Ltd., England. The material was chemically post-processed to provide the required crush strength.

### 3.2 Parameter Variation

For this study, the most significant parameters were investigated: The rotation about the z-axis (yaw angle), the impact height and the impact velocity. Table 1 shows an overview of the tests with the investigated parameters and their variation.

<b>Test No.</b>	<b>Parameter</b>
BAFGTR2-I4	<b>Reference Tests w/o Variation (previous project)</b>
BAFGTR2-I5	
BAFGTR2-I6	
BAFGTR2IA-10-1	<b>Z-Rotation -10°</b>
BAFGTR2IA-10-2	
BAFGTR2IA-10-3	
BAFGTR2IA10-1	<b>Z-Rotation +10°</b>
BAFGTR2IA10-2	
BAFGTR2IA10-3	
BAFGTR2IH-10-1	<b>Impact Height -10mm</b>
BAFGTR2IH-10-2	
BAFGTR2IH-10-3	
BAFGTR2IH-10-4	
BAFGTR2IH10-1	<b>Impact Height +10mm</b>
BAFGTR2IH10-2	
BAFGTR2IH10-3	
BAFGTR2IV-0.5-1	<b>Impact Velocity -0,5m/s</b>
BAFGTR2IV-0.5-2	
BAFGTR2IV-0.5-3	
BAFGTR2IV-1.0-1	<b>Impact Velocity -1,0 m/s</b>
BAFGTR2IV-1.0-2	
BAFGTR2IV-1.0-3	
BAFGTR2IV-1.0-4	
BAFGTR2IV0.5-1	<b>Impact Velocity +0,5m/s</b>
BAFGTR2IV0.5-2	
BAFGTR2IV0.5-3	
BAFGTR2IV1.0-1	<b>Impact Velocity +1,0m/s</b>
BAFGTR2IV1.0-2	
BAFGTR2IV1.0-3	

Table 1: Parameter Variations

## 4 Test Results

During this study a total of 25 tests were performed. Three tests were made for each parameter variation. The results of three reference tests without any parameter variation were taken from the previous evaluation test series with the same legform. Table 2 below shows an overview of all test results.

The raw data of the tests in ASCII format can be found in annex 3 of this report, the measurement data plots are presented in annex 4.

For the test numbers, the code of letters reads as follows:

BA = BAsT/ACEA

FGTR = Flex GTR

2 = Legform serial number

I = Inverse test

A = Angle variation

H = Height variation

V = Velocity variation

Test No.	Velocity [m/s]	Femur A3 [Nm]	Femur A2 [Nm]	Femur A1 [Nm]	Tibia A1 [Nm]	Tibia A2 [Nm]	Tibia A3 [Nm]	Tibia A4 [Nm]	ACL [°]	PCL [°]	MCL [°]	LCL [°]	Acceleration [g]	Temperature [°]	Parameter
BAFGTR2-I4	10,94	90,2	156,4	201,6	261,8	250,7	193,2	109,5	12,1	5,1	20,9	14,3	245,7	19,7	Reference tests w/o variation
BAFGTR2-I5	10,94	88,4	153	198,1	259,7	244,4	190,4	107,4	11,7	5	20,5	15,1	249,3	19,9	
BAFGTR2-I6	10,96	87,6	151,9	197,8	260,4	245,3	192,1	107,9	11,4	5,2	20,6	15,5	248,8	19,8	
BAFGTR2IA-10-1	11,18	79,5	138,3	189,2	268,3	246,0	190,0	108,0	9,8	5,3	19,9	12,0	249,2	20,5	Z-Rotation -10°
BAFGTR2IA-10-2	11,09	77,4	138,3	182,6	260,4	245,6	188,8	104,6	10,2	4,9	19,2	13,9	230,8	20,5	
BAFGTR2IA-10-3	11,17	78,1	137,8	182,9	264,1	244,7	187,7	106,0	10,1	4,8	19,3	13,4	237,2	20,7	
BAFGTR2IA10-1	11,09	81,1	141,3	189,1	264,6	245,4	186,7	105,2	10,4	5,2	19,9	13,6	239,0	20,6	Z-Rotation +10°
BAFGTR2IA10-2	11,03	81,8	139,8	187,5	261,0	246,4	189,7	105,7	10,8	4,8	19,5	10,1	236,2	20,8	
BAFGTR2IA10-3	11,05	79,5	139,0	187,2	269,7	250,9	192,3	106,4	11,2	4,8	19,4	14,9	242,7	20,9	
BAFGTR2IH-10-1	11,23	77,7	139,4	189,7	263,0	252,3	194,0	104,4	10,8	5,0	20,4	15,5	224,3	20,1	Height -10mm
BAFGTR2IH-10-3	11,12	76,8	137,0	190,6	268,1	253,9	194,1	105,1	9,4	4,9	19,4	13,8	230,6	20,4	
BAFGTR2IH-10-4	11,22	74,1	136,5	184,2	270,1	256,3	194,2	96,1	9,7	5,1	19,5	15,6	227,9	20,5	
BAFGTR2IH10-1	11,22	90,1	153,1	204,0	257,1	235,9	179,4	102,1	11,5	5,1	21,4	13,2	258,0	20,6	Height +10mm
BAFGTR2IH10-2	11,22	92,4	155,8	205,5	253,5	234,3	177,0	99,7	10,4	5,2	21,4	12,7	242,3	20,6	
BAFGTR2IH10-3	11,16	90,1	155,4	204,7	256,6	233,0	177,5	99,9	10,0	5,4	21,1	12,6	247,4	20,3	
BAFGTR2IV-1.0-1	10,14	67,5	127,0	169,7	245,2	235,0	179,2	98,7	10,1	4,2	17,7	12,4	228,3	20,4	Velocity -1,0 m/s
BAFGTR2IV-1.0-2	10,11	71,6	130,5	172,6	239,1	229,9	177,4	98,4	9,1	5,0	17,9	13,9	227,8	19,8	
BAFGTR2IV-1.0-3	10,08	78,4	135,6	174,5	236,1	224,3	174,4	98,7	9,3	4,6	18,4	11,5	230,8	20,3	
BAFGTR2IV-1.0-4	10,09	82,0	140,0	180,7	233,9	220,1	171,8	98,3	10,4	4,7	18,9	9,9	232,7	20,8	Velocity -0,5m/s
BAFGTR2IV-0.5-1	10,71	82,5	144,2	190,9	248,8	236,8	183,0	102,2	10,0	4,8	19,2	11,5	238,7	20,0	
BAFGTR2IV-0.5-2	10,70	76,3	138,8	185,3	252,0	237,9	184,4	101,7	10,8	4,8	19,0	11,1	244,9	20,2	
BAFGTR2IV-0.5-3	10,50	74,4	136,7	181,2	249,0	235,6	182,5	101,5	10,5	4,8	19,1	13,2	246,6	20,3	Velocity +0,5m/s
BAFGTR2IV0.5-1	12,01	80,4	147,9	199,1	283,0	264,0	203,7	115,0	11,1	5,4	21,2	14,3	254,6	20,1	
BAFGTR2IV0.5-2	11,97	82,7	150,7	202,6	282,9	257,6	200,0	112,5	10,6	5,7	21,2	13,8	238,8	20,0	
BAFGTR2IV0.5-3	11,89	86,6	154,3	206,1	279,0	262,2	200,0	110,8	11,0	5,4	21,2	14,4	262,9	20,2	Velocity +1,0m/s
BAFGTR2IV1.0-1	12,10	83,6	148,9	205,9	280,6	257,9	198,3	108,3	11,1	5,6	21,3	15,3	245,6	20,8	
BAFGTR2IV1.0-2	12,09	82,9	148,0	203,0	284,4	263,8	202,6	112,7	11,0	5,4	20,8	15,2	260,9	21,1	
BAFGTR2IV1.0-3	12,05	84,0	148,8	202,0	283,7	263,0	201,9	112,5	10,9	5,3	20,6	15,3	258,9	21,0	

Table 2: Overview of the test results

## 5 Evaluation of the Test Results

The main objective of this test series was the investigation of the influence of the test parameter variations on the test results.

Besides, since three repetitions were made with all test configurations, the repeatability of the test results under each parameter variation was also analysed. For this purpose, the coefficient of variation (CV) was calculated for every measurement channel in each test configuration. The rating used for the assessment of the repeatability is based on the best practice guidelines for dummies. The following classification is applied:

$$\text{Coefficient of Variation} = \frac{\text{Standard Deviation}}{\text{Mean Value}}$$

**CV < 3%: good**  
**CV 3% - 7%: acceptable**  
**CV 7% - 10%: marginal**  
**CV > 10%: not acceptable**

As the maximum value of LCL usually occurs during the rebound of the impactor, the CV value of this channel was not considered.

For the evaluation of the parameter influence the results of the reference tests without parameter variation were always used together with the results of the tests with parameter variation. To avoid a huge number of figures in this report, the column diagrams with the individual test results and with the averaged results are only presented in the annex.

The following figures show diagrams with the averaged test results and quantifications of the parameter influences. Since there will be no criteria for the femur bending moments in the gtr, only the results of the tibia bending moments and the knee elongations are shown.

The quantifications which are presented within the diagrams have to be seen with respect to the particular test configuration used in this study.

In addition to the results related to the objectives of this test series, some general observations and findings are also presented.

### 5.1 Rotation around the Z-Axis

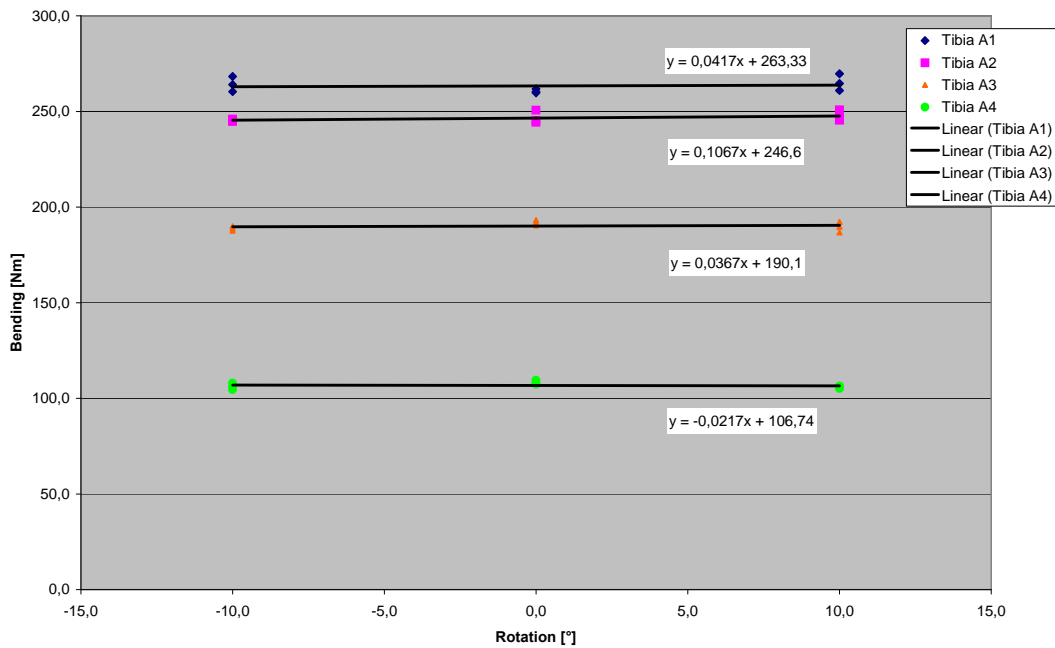


Fig. 10: Rotation around Z-axis: Tibia Bending Moments

In this graph no significant variation of test results seems to be visible. The tibia moment results appear to be not sensitive to a variation of the yaw angle.

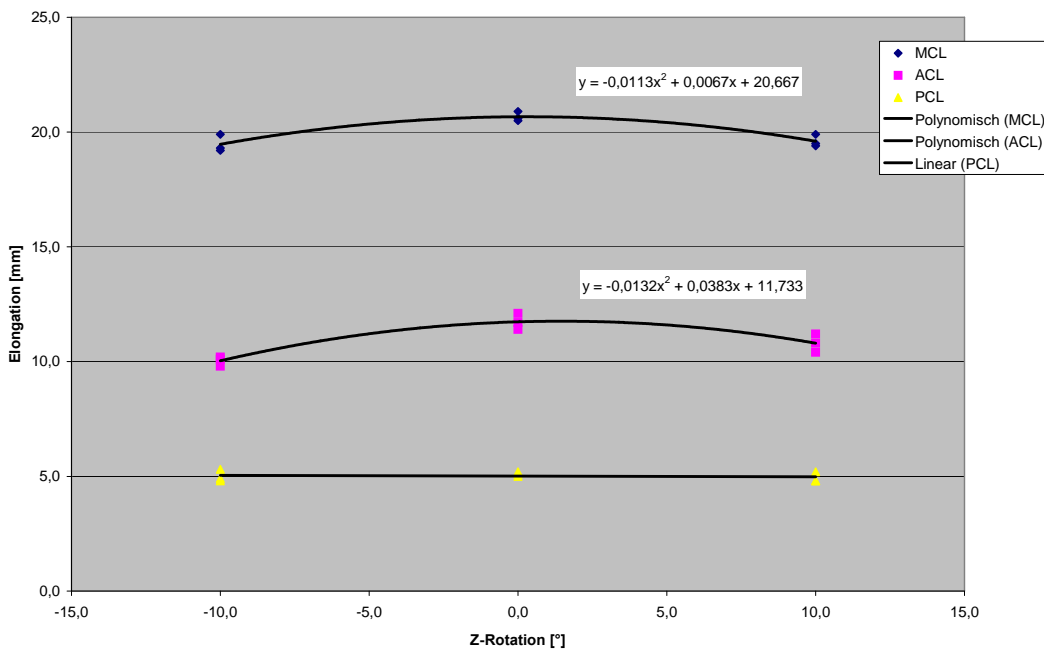


Fig. 11: Rotation around Z-axis: Knee elongations

This figure shows clearly that the results of MCL and ACL decrease significantly with an increase of the yaw angle, independent of its direction. However, the decrease is lower, especially for ACL, when the Z-rotation is +10° compared to -10°. In tests with an angle variation of -10° the results of MCL decrease by 6% and the results of ACL decrease by 15% whereas in

tests with an angle variation of +10° the results of MCL decrease by 5% and the results of ACL decrease by 8%. The reason for these differences is not obvious and requires further investigation.

The PCL results show no difference at all with this variation.

The coefficients of variation (CV) for the tibia and femur bending moments lie between 0,2% and 2,0%, which gives a “good” result for the repeatability. For the knee elongations, the CV was calculated to 1,4% - 5,3% which is at least “acceptable”.

## 5.2 Impact Height Variation

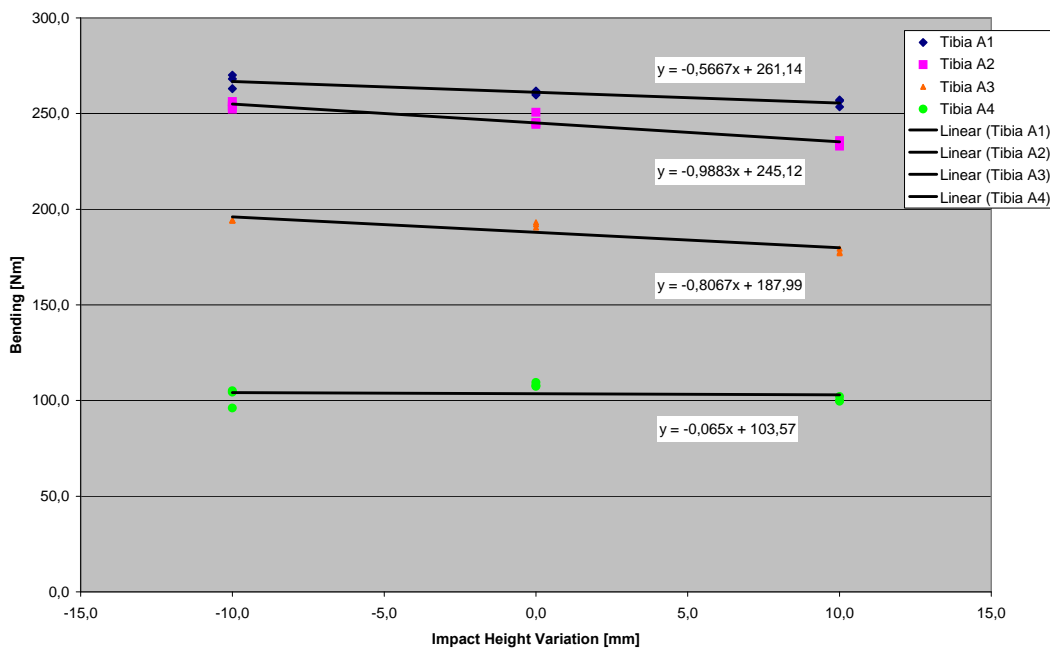


Fig. 12: Impact height variation: Tibia Bending Moments

From this graph, a clear tendency is visible at least for the first three tibia bending moments. The test results decrease with increasing impact height of the aluminium honeycomb. This effect is easily understandable because with increasing impact height the portion of the honeycomb that strikes the tibia directly becomes smaller, i.e. the energy introduced to the tibia becomes less. On the other hand, the femur bending moments increased with increasing impact height of the aluminium honeycomb.

In detail the decrease of the tibia bending moments is as follows:

- Tibia A1: -0,6 Nm / mm impact height
- Tibia A2: -1,0 Nm / mm impact height
- Tibia A3: -0,8 Nm / mm impact height
- Tibia A4: -0,1 Nm / mm impact height

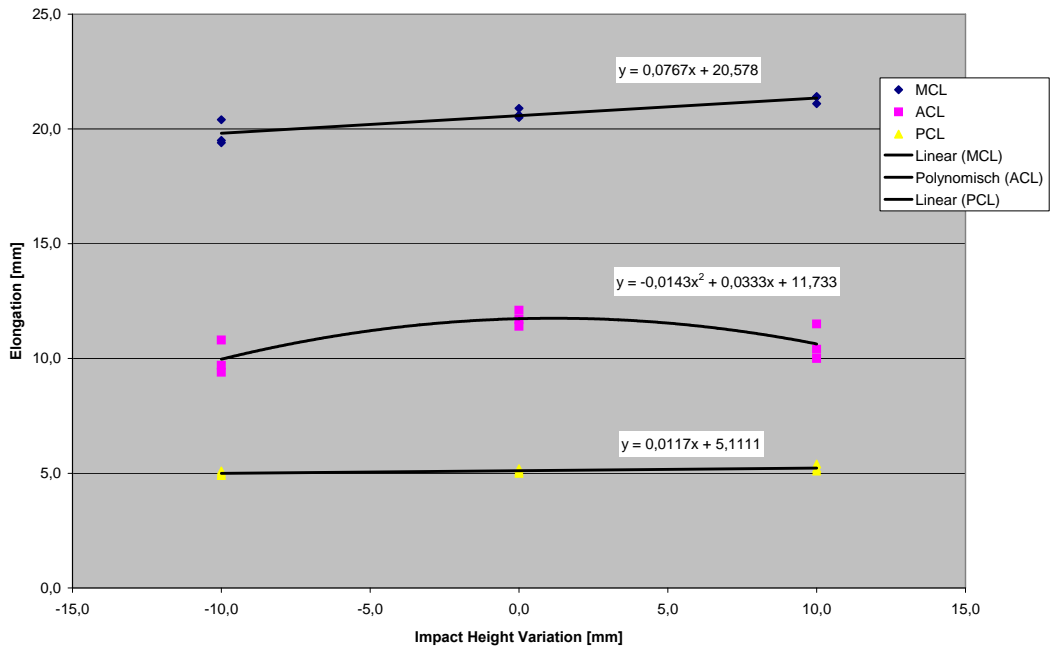


Fig. 13: Impact height variation: Knee elongations

Contrary to the tibia moments, the MCL results increase with increasing honeycomb impactor height. This also results from the position of the honeycomb relatively to the legform because with increasing impact height the portion of the honeycomb that directly hits the knee area increases, too. For this specific variation the averaged result increase lies by 0.08 mm / mm impact height. The maximum MCL value is expected in tests when the middle axis of the honeycomb is aimed to the centre of the knee.

The ACL results have their maximum in the original position and decrease by 15% for -10 mm impact height or by 9% for +10 mm. The obvious reason is that the original configuration (upper edge of honeycomb aims at centre of knee) introduces the maximum shear loading between upper and lower part of the knee. The reason for the differences between +10 mm and -10 mm is not clear.

The PCL results do not change significantly due to the height variation.

The coefficients of variation for this parameter variation are between 0,1% and 4,9% for the bending moments and between 0,8% and 2,9% for MCL and PCL, whereas for ACL the CVs are between 7,3% and 7,4%. This scatter may also result from the position of the honeycomb with its upper edge in line of the knee centre.

### 5.3 Impact Velocity Variation

The impact velocity is known to be a critical parameter which in case of a considerable deviation from the nominal value has a significant influence of the test results. Therefore, the variation investigation is based on two steps: nominal test velocity  $\pm 0,5$  m/s and  $\pm 1,0$  m/s.

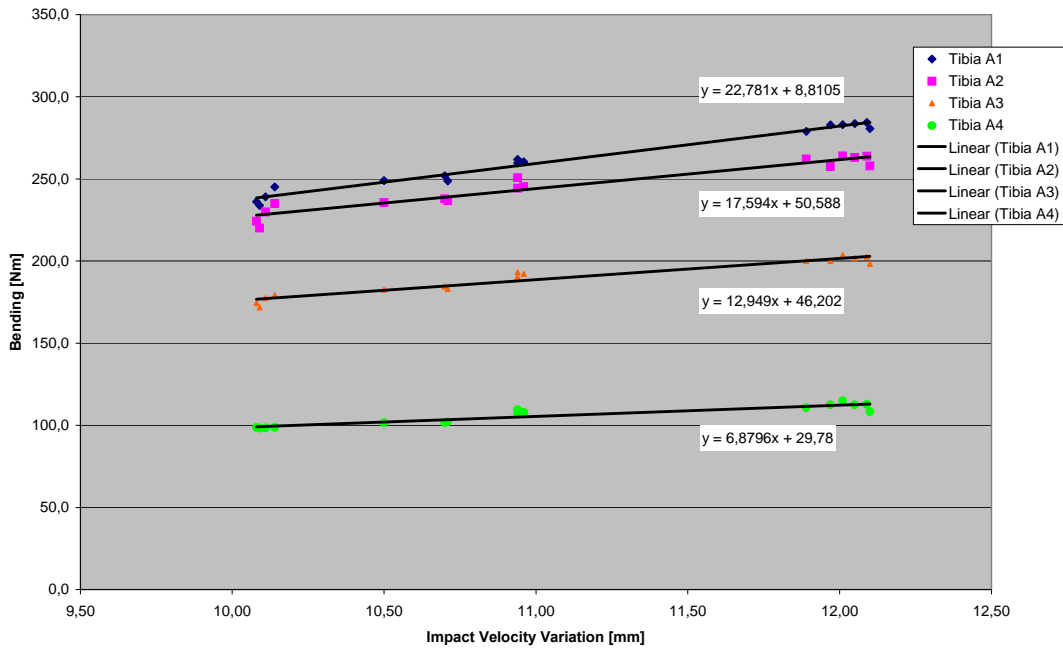


Fig. 14: Impact velocity variation: Tibia Bending Moments

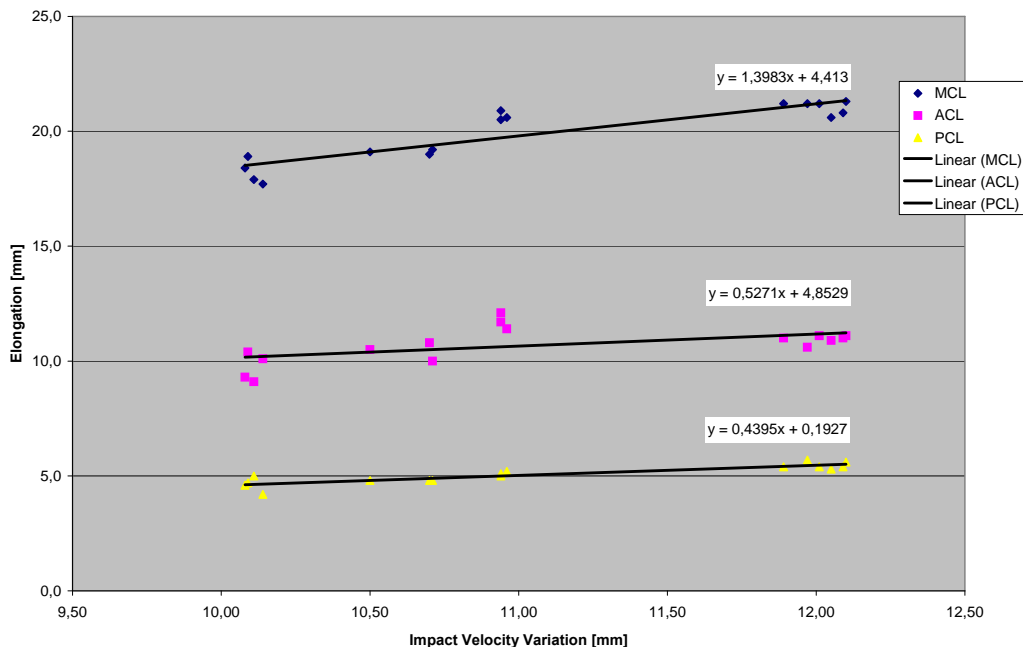


Fig. 15: Impact velocity variation: Knee elongations

As expected, all of the test results increase significantly with increasing impact velocity, because the higher velocity applies a higher load to the legform. The increase seems to be almost proportional for all of the measurement channels. The response of ACL is not entirely clear be-



cause in spite of the above mentioned tendency the maximum values were observed in the tests without velocity variation. The same effect was seen for the femur bending moments A2 and A3.

The increase quantifications are as follows:

- Tibia A1: +2,3 Nm / 0,1 m/s
- Tibia A2: +1,8 Nm / 0,1 m/s
- Tibia A3: +1,3 Nm / 0,1 m/s
- Tibia A4: +0,7 Nm / 0,1 m/s
- MCL: +0,14 mm / 0,1 m/s
- ACL: +0,05 mm / 0,1 m/s
- PCL: +0,04 mm / 0,1 m/s

The coefficients of variation were between 0.3% and 5.5% for the bending moments except Femur A3, which had a CV of 8.7% in the test with -1.0 m/s. The CVs for the knee elongations were between 0.0% and 3.9% except again for the test with -1.0 m/s where CVs between 3.0% and 7.1% were calculated.

#### **5.4 General Observations and Findings**

Since the parameter variations included tests with higher loadings (velocity) or oblique impact angles, this test series offered the possibility to look into the general performance of the legform under these particular conditions. Some general effects are remarkable:

- No damages of the legform including its instrumentation occurred during the tests
- No unexpected behaviour of the legform was observed
- No unexpected sensor output such as signal peaks were revealed

## **6 Conclusions**

Since generally the effects of the investigated parameter variations occurred as expected, the legform seems to have no hidden inconsistency.

The repeatability of the test results seems to be good or at least acceptable in most cases in spite of the parameter variations with oblique impacts or higher velocity.

The quantifications have to be seen with respect to the particular test configuration used in this study. However, the tendencies will most probably be similar for the majority of vehicle front designs.

Some details require further investigations:

- In tests with rotation around the z-axis the reason for different deviations with +10° and -10° was not clear and the effect when using higher values for the impact angle up to +/- 30° was not investigated.
- The analysis of effects of impact height variation should be expanded by impacting further upwards, e.g. centre of honeycomb in line with centre of knee or higher.
- During the impact velocity variation the ACL results posed an open question because the highest value was not in the test with the highest velocity.

The influence of other test parameters was not tested during this study and should be investigated in a subsequent project:

- Impactor rotation around X-axis
- Impactor rotation around Y-axis
- Ambient temperature

Furthermore the effect of a combination of parameter variations (e.g. impact height *and* impact velocity) will certainly be of some interest because the two effects of the individual parameter variations may boost each other or even cancel each other out.

## **7 Annexes (DVD)**

Annex 1: Photo documentation

Annex 2: Highspeed videos (AVI/MPG/JPG)

Annex 3: ASCII data of the tests

Annex 4: Measurement plots (PDF)

Annex 5: Datasheets of the sensors and honeycomb material used